# Computational design of S-Duct intakes for distributed propulsion

*Fabio Furlan, Nicola Chiereghin and Timoleon Kipouros*
Department of Power and Propulsion Sciences, School of Engineering, Cranfield University, Cranfield, UK
*Ernesto Benini*
Department of Industrial Engineering, University of Padova, Padova, Italy, and
*Mark Savill*
Department of Power and Propulsion Sciences, School of Engineering, Cranfield University, Cranfield, UK

**Abstract**
**Purpose** – The purpose of this paper is to identify efficient methods and tools for the design of distributed propulsion architectures.
**Design/methodology/approach** – Multi-objective computational aerodynamic design optimisation of an S-Duct shape.
**Findings** – Both duct pressure loss and flow distortion through such a duct can be reduced by wall-curvature changes.
**Research limitations/implications** – Initial simplified study requires higher fidelity computational fluid dynamics & design sensitivity follow-up.
**Practical implications** – Shape optimisation of an S-Duct intake can improve intake efficiency and reduce the risk of engine-intake compatibility problems.
**Social implications** – Potential to advance lower emissions impact from distributed propulsion aircraft.
**Originality/value** – Both the duct loss and flow distortion can be simultaneously reduced by significant amounts.

**Keywords** Design, Multi-objective optimisation, S-shaped diffuser, Genetic algorithm

**Paper type** Research paper



## Introduction

A substantial reduction of noise emission and drag is expected in future Blended-Wing-Body configurations (Liebeck, 2004), with propulsion systems highly integrated with the airframe, which require the installation of highly convoluted intakes. Curve intakes are characterised by adverse pressure gradient which is source of vortical structure and flow separation, with consequent swirl and not uniform distribution of total pressure at the inlet of the compressor (SAE, 1999, 2007; Wellborn and Okiishi, 1993). Loss of efficiency of the engine, unexpected stall and mechanical vibrations are direct consequence of distorted flow. To control separation and mitigate flow distortion, mechanical vortex generators and active jets were tested with encouraging results (Delot *et al.*, 2011; Gissen *et al.*, 2011).

This work aims to reduce flow distortion through optimisation of the intake shape by means of computational fluid dynamics (CFD) simulations and a multi-objective optimisation algorithm. Previous CFD shape optimisation of circular S-Duct suggested the possibility to obtain substantial reduction of flow distortion by localised deformation of the baseline geometry like bumps (Zhang *et al.*, 2000) and fin protrusions (Taskinoglu and Knight, 2004) or modification of the radius distribution along the axis (Bae *et al.*, 2012). This research is focussed on S-Duct with rectangular cross-section, more representative of a distributed propulsion application.

The proposed introduction of many distributed power devices towards the trailing edge of either a conventional civil airliner wing or next-generation blended-wing-body configuration provided the need to investigate and optimise sets of surface-aligned rectangular intakes with S-Duct geometry. The present work attempts to use CFD to optimise the S-curvature distribution for these to ensure maximum performance with minimum flow distortion into the engine face.

In the first instance, the S-Duct diffuser with a rectangular cross-section, as described by Paul *et al.* (2011), has been considered as the baseline for the optimisation design. The duct centre-line is defined by two circular arcs with identical radii, $R$ = 280 mm and angles, $\theta_{max}/2 = 30°$. The diffuser inlet is 65 × 65 mm and the outlet is 125 × 65 mm, giving an area-ratio ($A_r$) of 1.92. This configuration was previously experimentally investigated by Paul *et al.* (2011), by means of static pressure measurements on the lower and upper walls along the axis.

## Formulation of the optimisation problem

The formulation of the design case study is described in the following sub-sections, and the optimisation framework is presented in Figure 1. For the geometry management, six design variables have been considered (three for the upper curve and three for the lower one), subject to constraints on their horizontal and vertical movements. As a preliminary

The current issue and full text archive of this journal is available at **www.emeraldinsight.com/1748-8842.htm**

Aircraft Engineering and Aerospace Technology: An International Journal
86/6 (2014) 473–477

[DOI 10.1108/AEAT-04-2014-0046]

**Figure 1** Optimisation loop

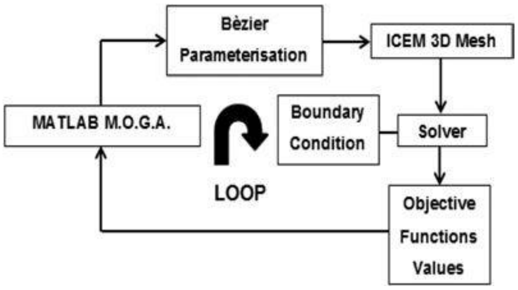


investigation, a total of 20 generations were executed with a population size of 24. The calculation of the objective functions of each individual took 1 hour. As optimiser, the Matlab multi-objective optimisation toolbox, was used, which implements an elitist variant of the NSGA-II algorithm.

## Geometry parameterisation

Parameterisation with Bézier control points, minimising error between the datum coordinates and a temporary geometry at every step of convergence, has been adopted because this technique should allow adequate exploration of design space, but is sufficiently simple to limit the number of decision variables required for speed of optimisation.

The main features of the implemented parameterisation scheme, illustrated in Figure 2, are as follows:

- the length and the offset of the duct are fixed by the first and fifth control points;
- the second control point is also fixed, relative to the first, to guarantee a tangential condition at the inlet and ensure continuity of the first derivative;
- the third control point is free to move in both *x* and *y directions*, in the central, change of curvature region and close to the initial separation zone; and
- the fourth control point is allowed to move in the *x direction* only to satisfy the tangential condition at exit:

$$\frac{\Delta Y_1}{\Delta X_1} = \frac{\Delta Y_2}{\Delta X_2} \tag{1}$$

The design vectors are controlled by hard geometrical constraints to maintain a realistic shape of the duct, well as

**Figure 2** S-Duct parameterisation

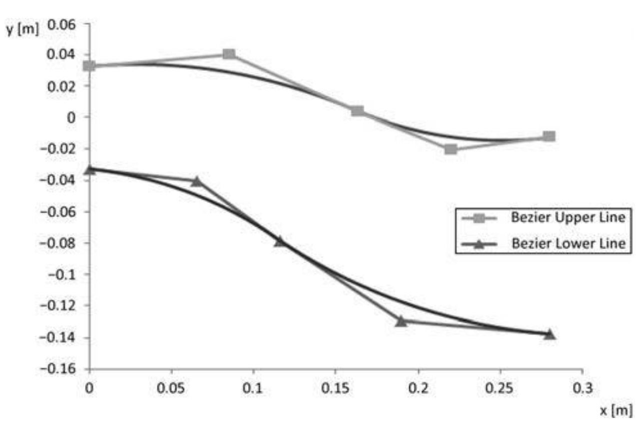


tangential conditions at the inlet and between the two parts of the S-curve.

## CFD meshing and modelling

ANSYS ICEM has been used to generate an initial mesh; the flow domain was extended upstream and downstream of the inlet and the outlet of the duct, by an amount equal to the duct length ($L$ = 410 mm), as illustrated in Figure 3. This ensures that a developed boundary layer is established at the inlet of the duct; allows a static pressure condition to be applied at the outlet; and avoids any problems associated with possible flow reversal there. To reproduce the experimental condition by Paul *et al.* (2011), and simplify the mesh generation during the optimisation loop, the transition between rectangular and circular sections (for the compressor inlet) is not consider in this report. According to the experimental flow conditions, the inlet velocity is set to 33 m/s with a Reynolds number of $1.34 \times 10^5$.

For the current adiabatic and incompressible flow, a *Mass-Flow-Inlet* condition and *Pressure-Outlet* condition were applied, and the *pressure–velocity coupling*, *SIMPLE*, numerical solution scheme was adopted. This was adequate for capturing the experimental conditions as the Mach number was below 0.3.

Five different turbulence models were tested, and the realizable k-epsilon variant was found to provide the best fit to experiment for the datum design (Figure 4), at a relatively course mesh resolution of 500,000 cells found from a separate mesh refinement investigation to provide adequate accuracy with sufficient speed for design optimisation.

## Objective functions

Two flow metrics that express the efficiency of S-Duct diffusers were defined as the relevant objective functions for simultaneous minimisation in the multi-objective optimisation problem:

- An area-averaged coefficient of total pressure loss, $C_{ploss,avg}$:

$$C_{ploss,avg} = \frac{P_{t,\infty} - P_{t,outlet,avg}}{q_\infty} \times 100 \tag{2}$$

where, $P_{t,\infty}$ is the inlet total pressure, $P_{t\_outlet,avg}$ is the total pressure at outlet and $q_\infty$ is inlet dynamic pressure:

**Figure 3** S-Duct computational model

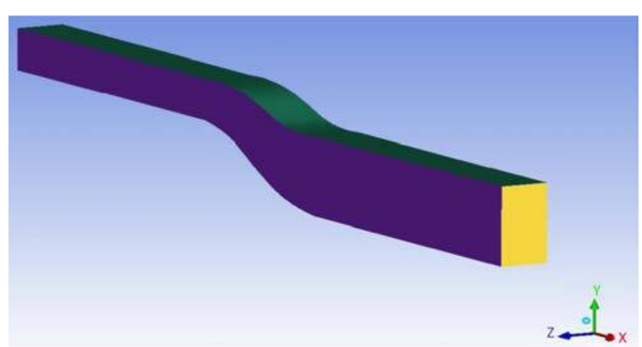

- A distortion coefficient, *DC*, representing the flow distortion at the engine face. A cross-sectional plane 65 mm (inlet section edge) downstream of the S-Duct outlet is divided into six sectors of equal area. The distortion coefficient is calculated as the difference between average total pressure of the whole plane and the average value in the sector with the highest total pressure deficit, normalized with the inlet dynamic pressure:

**Figure 4** Turbulence models sensitivity study

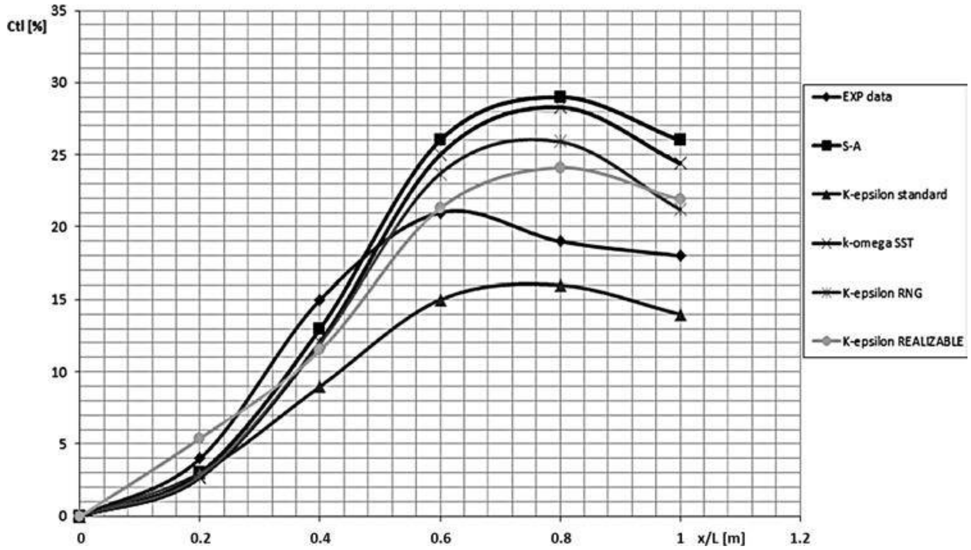


**Figure 5** The Pareto front (left), and optimised shapes (right)

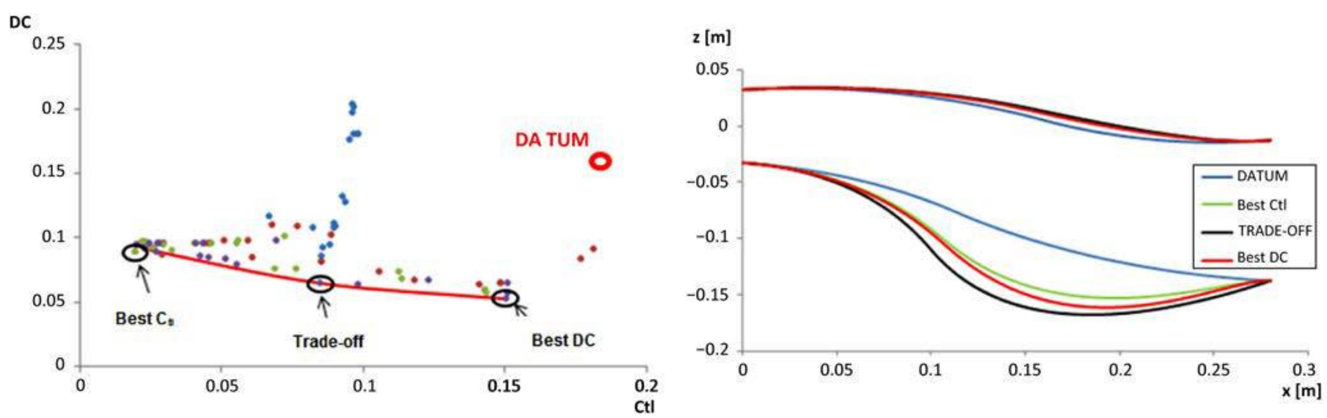


**Figure 6** Three-dimensional representation of the baseline (left) and optimized (right) configurations

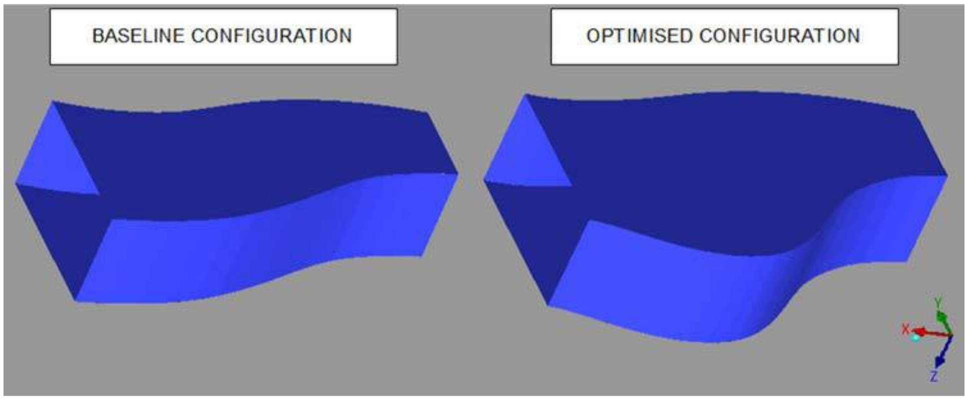

$$DC = \frac{P_{t,outlet,avg} - P_{t,\min,avg}}{q_\infty} \times 100 \qquad (3)$$

This definition differs from the standard DC(60) definition (Bissinger and Breuer, 2010) to be adapted to the rectangular section of the S-Duct outlet.

## Results and analysis

The evolution of the S-Duct design and the Pareto front found after 20 generations can be seen in Figure 5(left). The corresponding geometrical shapes for three selected optimum designs are shown in Figure 5(right). The trade-off solution expresses the largest changes in the geometry. A three-dimensional comparison between baseline and optimized geometry is outlined in Figure 6, where a remarkable difference is observed in the lower wall, with a large bump before the outlet in the optimized configuration.

**Figure 7** Total pressure distribution at the S-Duct outlet for datum (left) and optimized (right) configurations

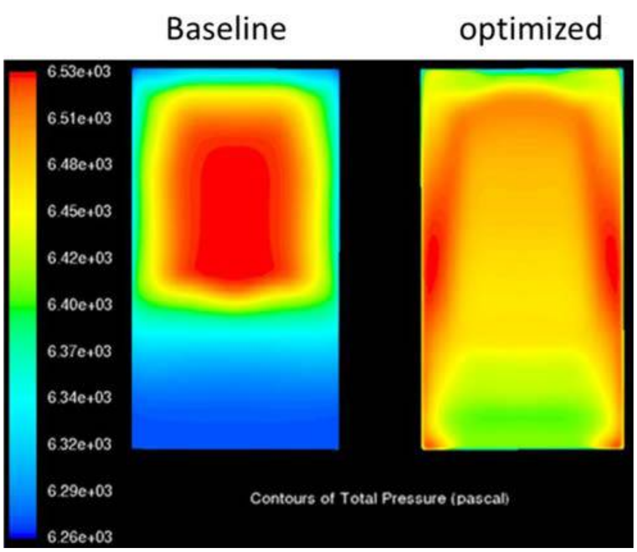


Figure 7 shows the total pressure distribution on the cross-section at the S-Duct outlet. A more uniform distribution for the optimized case (right) in comparison with the baseline (left) is evident.

In Figure 8(left), a vortex region near the upper-line can be appreciated at the inlet section. This is a separation zone induced from the curvature change which pushes the flow inwards to the centre of the duct, inclining the stream-lines and creating a stream-tube approximately with the same inlet area section, thus postponing the diffusion. After the first bend, on the lower-line, the flow separates, generating a vertical flow which prevents the adverse pressure gradient from causing a second separation and therefore ensuring the flow adheres to the lower wall. The flow field is thus now characterised by secondary flows only in the first half of the S-Duct and not by vortices produced from the lower wall, so there is no longer a shift of the flow upwards in the second half, or the creation of two zones of different momentum at the outlet section. Instead, after the first curvature, the flow follows the lower-line until a bump associated with high static pressure causes the flow to deviate and accelerate. The progressive decrease in the cross-section of this bump increases the velocity approaching the outlet, as can be seen in Figure 5(right). These effects create a flow control inside the duct, reducing the total pressure distortion at the outlet.

## Conclusions

After determining an adequate turbulence model and grid resolution, the upper and lower surface curvature shapes of a rectangular area-ratio S-Duct have been optimised for minimum pressure loss and outlet flow distortion under the additional constraints of fixed duct length and off-set. Three resulting optimal designs have then been evaluated, and the reason for the best compromise performance assessed in terms of associated changes in duct flow topology. The results suggest that multi-objective design optimisation can be usefully employed to help define designs for candidate distributed propulsion engine intakes.

**Figure 8** Streamlines (left) and velocity vectors (right), coloured by static pressure

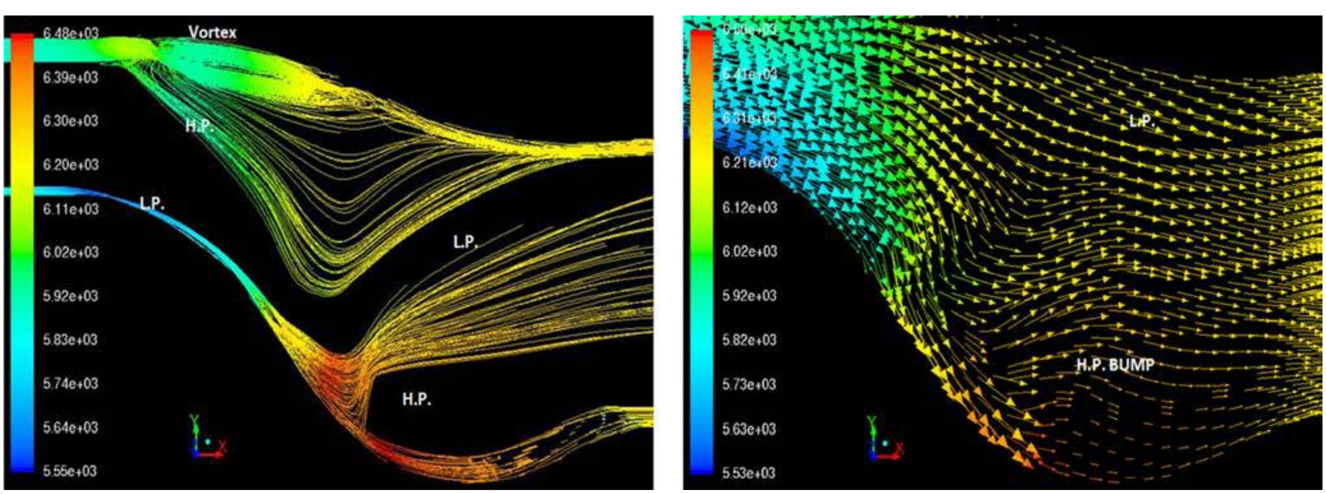

Aircraft Engineering and Aerospace Technology: An International Journal
Volume 86 · Number 6 · 2014 · 473–477

## References

Bae, H., Park, S. and Kwon, J. (2012), "EGO method for diffusing S-Duct shape design", *Seventh International Conference on Computational Fluid Dynamics (ICCFD7), ICCFD7-2401*, *Big Island, HI*.

Bissinger, N.C. and Breuer, T. (2010), "Basic principles - gas turbine comptatibility - intake aerodynamics aspects, in" Blockley, R. and Shyy, W. (Eds), *Encyclopedia of Aerospace Engineering,* Vol. 8, Chapter EAE487, Wiley & Sons, River Street, Hoboken, NJ.

Delot, A.-L., Garnier, E. and Pagan, D. (2011), "Flow control in a high-offset subsonic air intake", *47th AIAA/ASME/SAE/ASEE Joint Propulsion Conference & Exhibit, AIAA 2011-5569*, *San Diego, CA*.

Gissen, A.N., Vukasinovic, B., McMillan, M.L. and Glezer, A. (2011), "Distortion management in a BLI inlet diffuser using synthetic-jet hybrid flow control", *AIAA Paper 2011-35*, *Orlando, Florida*.

Liebeck, R.H. (2004), "Design of the blended wing body subsonic transport", *Journal of Aircraft,* Vol. 41 No. 1, pp. 10-25.

Paul, A.R., Kuppa, K., Yadav, M.S. and Dutta, U. (2011), "Flow improvement in rectangular air intake by submerged vortex generators", *Journal of Applied Fluid Mechanics,* Vol. 4 No. 2, pp. 77-86.

SAE (1999), *Inlet Total-Pressure-Distortion Considerations for Gas-Turbine Engines*, No. AIR1419, Society of Automotive Engineers, Warrendale, PA .

SAE (2007), *A Methodology for Assessing Inlet Swirl Distortion*, No. AIR5686, Society of Automotive Engineers, Warrendale, PA.

Taskinoglu, E.S. and Knight, D.D. (2004), "Multi-objective shape optimization study for a subsonic submerged inlet", *Journal Of Propulsion and Power,* Vol. 20 No. 4.

Wellborn, S.R. and Okiishi, T.H. (1993), "A study of the compressible flow through a diffusing S-Duct", NASA Technical Memorandum 106411.

Zhang, W., Knight, D.D. and Smith, D. (2000), "Automated design of a three-dimensional subsonic diffuser", *Journal Of Propulsion and Power,* Vol. 16 No. 6.

## Corresponding author

**Timoleon Kipouros** can be contacted at: timos.kipouros@cranfield.ac.uk